Uniport Journal of Engineering and Scientific Research (UJESR)

Vol. 8, Issue 2, 2024, Page 346-363
ISSN: 2616-1192

(www.ujesr.org)

PV-Wind Hybrid Electricity Supply System for Remote Communities in Rivers State: A Techno-Economic Approach

Humphrey Ibifubara
Department of Physics, University of Lagos, Nigeria.
Corresponding author's email: ihumphrey@unilag.edu.ng

Abstract
This study evaluated the feasibility and economic viability of a hybrid electricity supply system that combines photovoltaic (PV) solar and wind energy to power remote communities in Rivers State. HOMER (Hybrid Optimization of Multiple Energy Resources) software was utilized for this analysis. The hybrid system integrates the XANT M-21-ETR Wind Turbine, SMA Sunny Tripower 60-US inverter with Generic PV modules, and the LG Chem RESU10 battery for energy storage, ensuring a consistent energy supply even during periods of low renewable generation. Through a comprehensive techno-economic analysis, the system's performance was optimized to meet the AC primary load requirements, averaging 160 kW. Sensitivity analysis, which incorporated fluctuations in expected inflation rates of 5%, 10%, and 15%, underscored the influence of economic variables on the financial performance of the system. Net present cost (NPC) of the system was estimated to be between $1.5 million and $2 million, influenced by fluctuations in inflation rates and sensitivity factors such as changes in wind speed, solar irradiance, and maintenance costs. In conclusion, the optimized PV-wind hybrid system, backed by cutting-edge storage solutions, presents a sustainable and economically feasible method for electrifying remote communities. The novelty of this study arises from its incorporation of renewable energy technology, its application specifically tailored to the circumstances of isolated settlements in Rivers State, and its consideration of both technical and economic aspects. These factors may render it a reproducible model for other off-grid locations.

Keywords: *Photovoltaics, Wind turbine, Sensitivity factor, Optimization, Sustainability, Hybrid*

Received: 1st November, 2024 *Accepted: 31st December, 2024*

1. Introduction

Several of the SDGs, including eradicating poverty, improving health, education, access to clean water, industrialization and climate protection, rely on having a source of affordable, reliable and sustainable energy. However, the availability of energy varies greatly across nations, and current development is insufficient to meet the requirements of Sustainable Development Goal 7 (SDG 7). Increased efforts will be required, particularly in countries with severe energy bottlenecks and high energy consumption. Lack of availability of energy and transformation systems impede human and economic development, since access to power is necessary for development. Energy consumption is increasing due to global population growth and increasing industrialization, but conventional energy sources cannot keep up with this demand. Increased use of fossil fuels without addressing the issues of hazardous gaseous emissions, high fuel life cycle costs and greenhouse gas mitigation activities would have implications for global climate change (Giannetti et al., 2020). Renewable energy sources are abundant, inexhaustible and environmentally friendly. Solar, wind, hydroelectric, geothermal, biofuels and other renewable energy sources are available in the environment. Energy efficiency and the increased use of renewable energies reduce CO_2 emissions, contribute to climate protection and minimize the risk of disasters (Wang et al., 2022).

In developing countries, access to energy is often relatively limited. Incredibly, 8.4% of South Asians and a stunning 52.3% of people in sub-Saharan Africa do not have a source of power (IEA, 2019a; World Bank, 2020a). About 10.4% of the world's population does not have access to electricity. Based on 2023 World Bank assessment, 40% of those having access have less than 12 hours of daily utility power. This has left households in rural areas

at greater danger. According to WHO (2016), the World Bank (2023), more than 82% of rural residents in Sub-Saharan Africa still use kerosene lamps and candles for illumination and conventional firewood stoves for cooking.

The International Energy Agency (IEA) projects that there will be 2.8 billion traditional stove users worldwide by 2030, up from 1.7 billion in 2010 (IEA, 2010). By 2030, the agency predicts this will cause more than 1.5 million deaths annually. Globally, 3.8 million people died from related diseases as of 2018, with 27% of those deaths from pneumonia in children under five, chronic obstreperous respiratory disease, and stroke, cancer of the lung, ischemic heart disease, and 8% of all deaths (WHO, 2020). More than 40% of Nigeria's population or 87.4 million people have no access to electricity. For lighting and cooking, 58% of people use kerosene and 57% firewood (World Bank, 2019; IEA, 2023c). Only 10% of people can cook clean. Nigeria needs about 98,000 MW of energy annually. However, around 4,000 MW are produced for the 110 million grid-connected users (Maren et al., 2024). According to Nigeria's Energy Profile, the nation has a total installed capacity of 12,522 MW and a total transmission capacity of 8,100 MW (USAID, 2020).

Electricity is essential for people's life and livelihood. It powers everything from homes and schools to local communities, allowing us to store groceries and medicines in freezers and keep our phones charged so we can stay connected. Many rural communities in Nigeria do not have access to electricity and few can afford the costly diesel-powered generators that pollute the environment and endanger people's lives. Solar-powered mini-grids are a great way for rural communities to meet their electrical demands (Akinyele, 2018). They work well for small, isolated villages. Mini-grids powered by renewable energy are getting more and more economical and ecologically friendly. Grid extension, free-standing solar panels and mini-grids are three options for rural electricity. The system expansion connects people and cities that are currently not connected to the national power grid. Large, densely populated communities living close to the power grid can be connected cost-effectively; however, the cost of expansion increases exponentially with increasing population density (Vendoti *et al*., 2018). Off-grid, stand-alone solar systems can provide power for necessities such as lighting and phone charging in remote areas where grid expansion is impractical. However, they are not designed for larger performance requirements such as operating machinery or agricultural equipment.

Solar and wind-based generation technologies are especially long-lasting and environmentally friendly options for providing electricity for isolated areas. These technologies can be effectively utilized for residential, off-grid, and commercial purposes, offering numerous benefits (Saha *et al*., 2022). Solar energy conversion and storage systems have developed as an incredibly appealing alternative to power supply, despite having a high-power price per kWh and a small efficiency in converting energy. On the other hand, the output of wind energy has increased significantly. Though the profitability and ideal size of wind turbines have been the subject of numerous studies (Anigbata et al., 2022; Gul *et al.*, 2022). The main disadvantages of solar and wind energy are their stochastic natures, which cast doubt on the reliability of the electricity delivered to the end user. Therefore, integrating solar and wind power is a practical way to improve reliability, such that the strength of one can make up for the deficiencies of the other. Several studies have been conducted on the feasibility of self-sufficiency with solar-wind hybrid energy systems (Das et al., 2016; Balachander *et al*., 2021). Another disadvantage of a standalone solar-wind power system is its reliance on a backup power source due to the unpredictability of solar and wind resources. However, solar-wind hybrid systems are economical, dependable and offer environmental benefits such as reliable power supply and greenhouse gas emission reduction for rural electrification (Khalil *et al*., 2021). Solar energy alone has been shown to be more cost-effective for supplying rural areas. Solar/wind/storage systems have proven to be the most cost-effective option for autonomous power generation in off-grid environments. A grid-connected system uses less energy than a system that's disconnected from the grid for a given load requirement (Li *et al*., 2020). For remote power supply, an off the grid hybrid system is less expensive and is more dependable than one power source. According to the sustainability analysis, reducing grid capacity for charging batteries would enhance the renewable share. When the system is connected to the network, it is less expensive than off the grid methods (Fulzele and Daigavane, 2018; Dash, *et al*., 2023).

Hybrid energy solutions are proposed in this study for all fishing communities in Asari-toru, L.G.A, Rivers State, Nigeria (popularly called

fishing port) that are not yet electrified. These areas are relatively far away from the grid. In addition, using a diesel generator is impractical due to the difficult access to fuel. The distance from Elem-Ifoko to Port Harcourt, where the nearest petrol station is located, is 47.8 kilometers. The feasibility of hybrid energy systems has not yet been investigated for the study area. The primary purpose of this article is to serve as a guide to electrifying remote fishing ports in Rivers State through the use of sustainable energy sources. A hybrid solar-wind energy solutions are modelled in this paper using the application Hybrid Optimization Model for Electric Renewables (HOMER) with hypothetical Elem-Ifoko load profiles.

2. Materials and methods

2.1 Study areas

Elem-Ifoko is a fishing settlement located at a remote region of Rivers State. Rivers' capital Port Harcourt is approximately 47.8 km / 30 miles away from Elem-Ifoko. Geographical coordinate is Latitude 4°25'40.3"N Longitude 6°59'44.7"E. Other fishing settlement within 5 km around Elem-Ifoko are Egele, Odumo, Elem Abalamo, Elem-Agbalama, Elem-Krakrama, Elem-Tombia, Dariama, Elem Benkinkiri, Mbiakafiama, Lelema. All these settlements have no electricity because it is not feasible to construct a grid-connected system from nearest station to the location. However, the location is near the Gulf of Guinea and the South Atlantic Ocean, as such renewable energy such as wind and solar energy are readily available. The settlement has over 100 households and a population of over 500 people. The occupation of the people who live there are trading, farming and fishing. Because there is no electricity, the people rely on wood biomass. A hybrid power system with multiple renewable energy sources may provide consistent and continuous electricity generation. This research study discussed the sustainability of a hybrid power generation system using natural and cost-effective analysis. The analysis was done on the minimal operations of a hybrid power generating system that produces 157 kWh per day as a stand-alone power generation system using solar panels and wind turbines. A renewable energy-based system has been suggested to provide electricity to the settlement. The map of the study area is shown in Fig. 1.

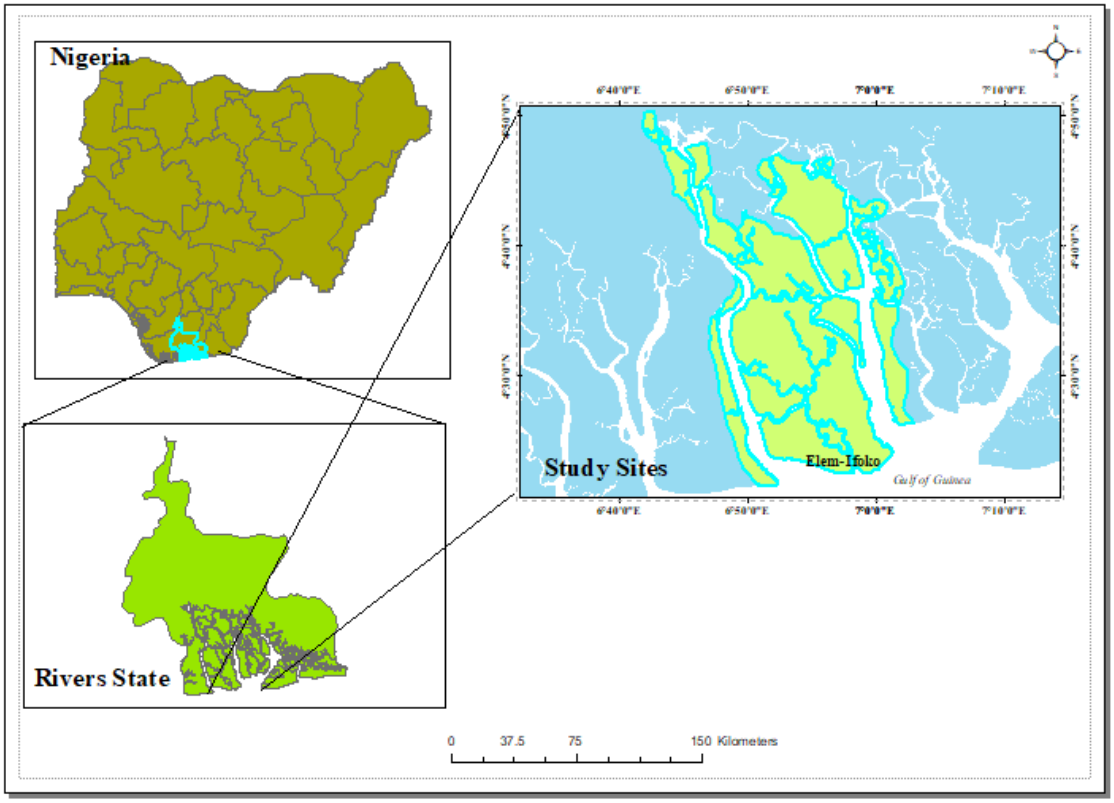

Fig. 1: Study area map of Elem-Ifoko fishing settlement in Rivers State

2.2. Electricity demand assessment

A hybrid wind-solar power system is proposed for the location, consisting of a typical 100kW wind energy generator and 60kW photovoltaic panels with storage and a converter, as represented by the system devices in Fig. 2.

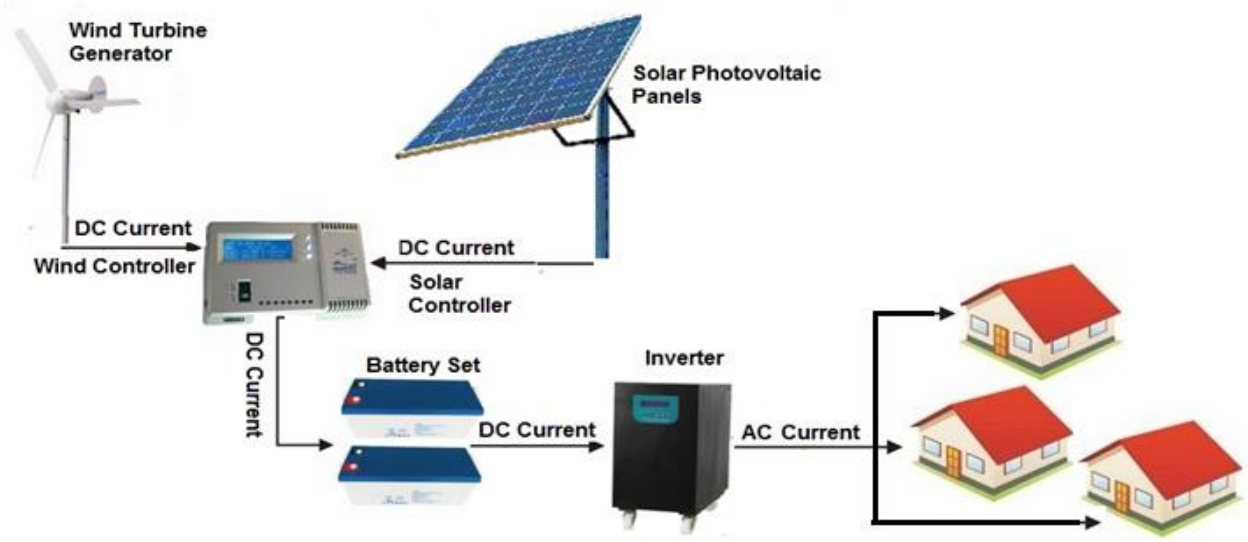

Fig. 2: The basic schematic for the proposed hybrid wind-solar power system

2.2.1 Wind turbine system

The average power production characteristic of a wind turbine changes depending on the manufacturer's decisions. Wind turbines start generating electricity at their switch-on speed. As they accelerate to their rated speed, the power output continues to increase. It should be noted that the power curve of wind turbines, which describes the relationship between the power produced by the turbine and a speed (Sarkar and Khule, 2016; Tigabu et al., 2019), is one of its most important aspects. Equation (1) can be used to express the total annual wind turbine power (W_P) in (kWh) produced:

$$W_P = \sum_{t=1}^{N_h} N_t P_t(v_t) \quad (1)$$

where (N_h) represents the number of data hours in a year, (t) represents the hour of the year, (P_t) represents the power production in (kW) as a function of the average wind speed for a particular hour, and (N_t) represents the number of turbines at the location (Alsharif, 2017). Equation (2) states the relationship between the wind power output (P_w) in (kW) and the air density (ρ_a) (1.23 kg/m^3), the wind turbine rotor swept area (A) in (m^2), the coefficient wind turbine power (C_p), the velocity of the wind (V_r) in (m/s), the efficiency of the wind turbine (η_t) and the efficiency of the wind generator (η_g).

$$P_w = \tfrac{1}{2}\rho_a A C_p V_r^3 \eta_t \eta_g \quad (2)$$

2.2.2 Photovoltaic system

The total power (S_P) produced annually by a photovoltaic system in (kWh) can be calculated using the relationship in Equation (3). Where N_h denotes the number of data hours per year, t is the hour of the year, the solid area of the solar field (A_{solar}) in (m^2), the hourly insulation (S_t) in (Wm^{-2}) and the efficiency of the solar system (η_{solar}, t) for a given hour of the day for a given month (Reichling and Kulacki, 2008).

$$S_P = \sum_{t=1}^{N_h} \eta_{solar,t} A_{solar} S_t \quad (3)$$

The relationship in Equation (4) expresses the output power (P_{pv}) of the photovoltaic array in (kW). Where Y_{pv} is the nominal capacity of the solar system in (kW), i.e. the power production under Standard Test Conditions (STC), and K_{pv} is the percentage of the derating factor of the photovoltaic system. $I_{S,\,STC}$ represents the incident solar irradiance at STC (1 kW/m^2), I_S represents the incident solar irradiance on the PV array at the current time step in (kW/m^2), Tpv, STC represents the temperature of the photovoltaic cell at STC,

which is 25 °C, Tpv represents the temperature of the photovoltaic cell at the current time step in (C), and α_P represents the power temperature coefficient in (%/C) (Fantidis *et al*., 2015; Sanni *et al*., 2016).

$$P_{pv} = Y_{pv}.k_{pv}\left[\frac{I_S}{I_{S,STC}}\right]\left[1+\alpha_P\left(T_{pv}-T_{pv,STC}\right)\right] \quad (4)$$

The relationship given in Equation (5) determines the total annual power in (kWh) gotten from the hybrid renewable system (H_P), which is the sum of the total annual wind turbine power (W_P) and the total annual power generated (S_P) by a photovoltaic system (Sofimieari *et al*., 2019)

$$H_P = W_P + S_P \quad (5)$$

2.3 Model for HOMER program simulation

The National Renewable Energy Laboratory in the United States (NREL) developed the hybrid optimization model for electric renewables (HOMER) as a computer model to assist designers in creating renewable energy systems for both ON-grid and OFF-grid projects and to make it simpler to evaluate power generation technologies through a wide range of combinations (Lilienthal and Lambert, 2004; Givler and Lilienthal, 2005). Fig. 2 illustrate the hybrid power model created using the HOMER program, respectively. A 100 kW XANT21 wind turbine, a 60 kW SMA60-US PV flat panel, an electronic converter, 40 LGChem RESU10 (9.8kWh) batteries, and a community load make up this model.

2.3.1 Load demand profile

A 500-person village with 100 houses, a market, two schools (elementary school and high school) and a church was studied to calculate the main electrical load. Two energy efficient lamps (5W each), two fans (100W each) and a colour TV (70W each) were considered for each household. Each school has eight lights and eight fans while the church has four lights and four fans. The majority of time is spent on lights, colour television, and fans, which take up 9 hours, 5 hours, and 6 hours every day, respectively. A general load centre with a daily average requirement of around 157 kWh is considered. The load in this analysis is presented with some peak demands of almost 22.18 kW and a load factor of 0.295, or the average power divided by the peak power over a 24-hour period (Figure 3). The community load profile, the insolation profile and wind speed profile for the Elem-Ifoko fishing community in Rivers State, Nigeria are shown in Fig. 4, 5 and 6, respectively.

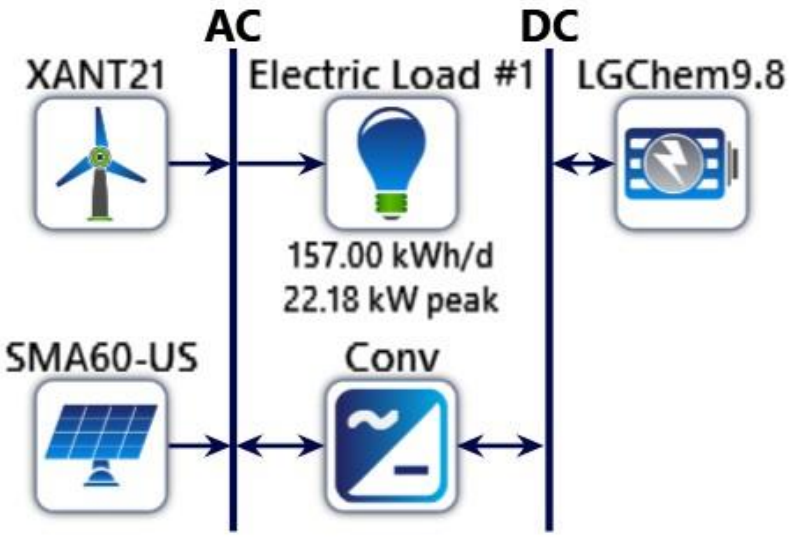

Fig. 3: Proposed hybrid power generation system in homer software

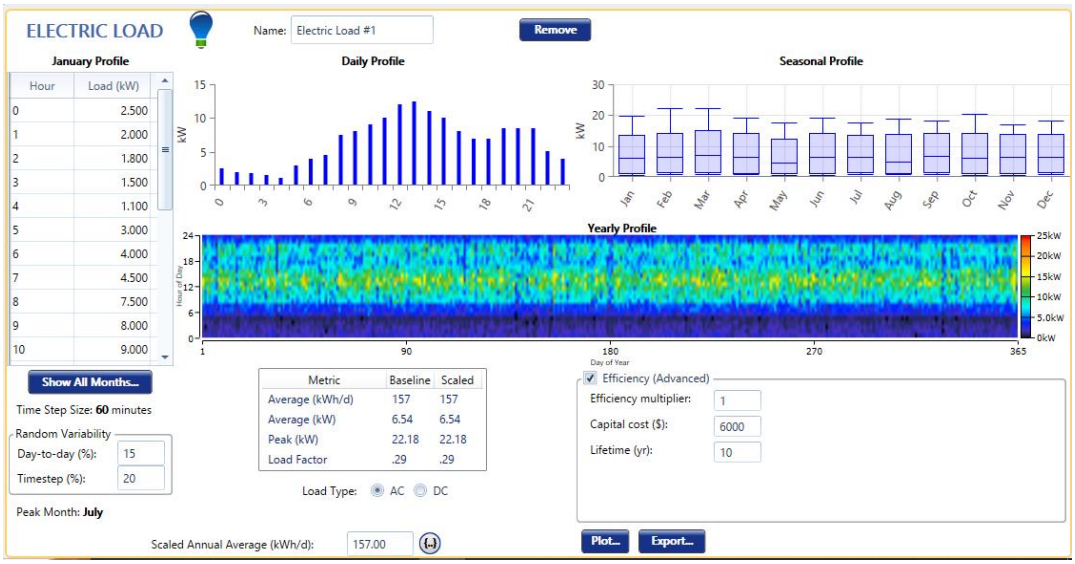

Fig. 4: Proposed Hybrid System Load Profile of Elem-Ifoko fishing settlement in Rivers State, Nigeria

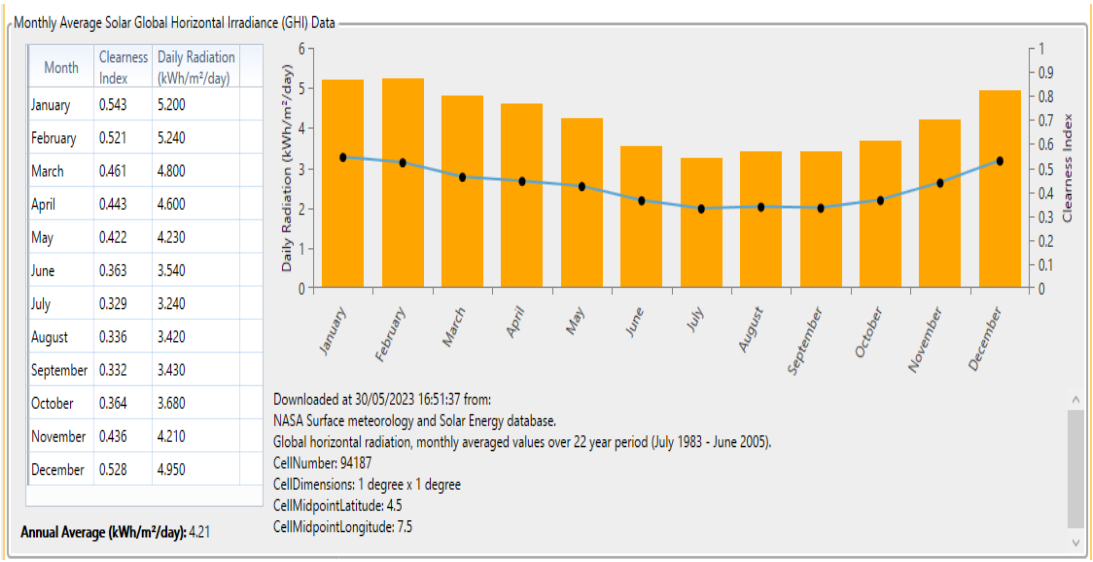

Fig. 5: Solar resources profile of Elem-Ifoko fishing settlement in Rivers State, Nigeria

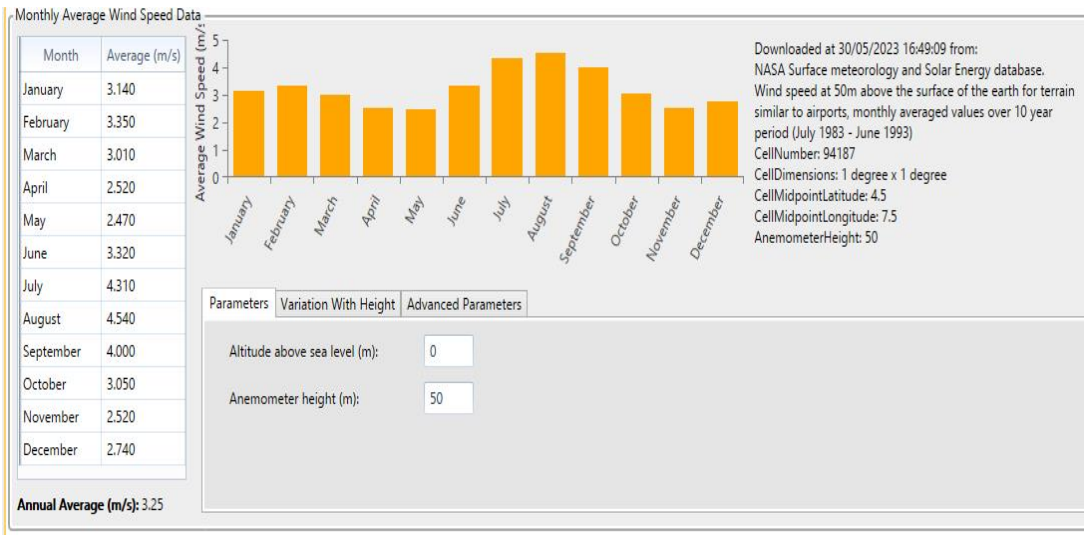

Fig. 6: Wind speed profile of Elem-Ifoko fishing settlement in Rivers State, Nigeria

Fig. 7 illustrates the annual energy output of the wind-solar hybrid system with diurnal and seasonal trends. The power output is depicted using a colour scale from low (dark blue) to high (red) in kilowatts (kW). Highest energy production is witnessed during the day while wind energy steps in during nights or during periods of low solar irradiation, thus demonstrating the potential of complementary energy production from wind and solar power.

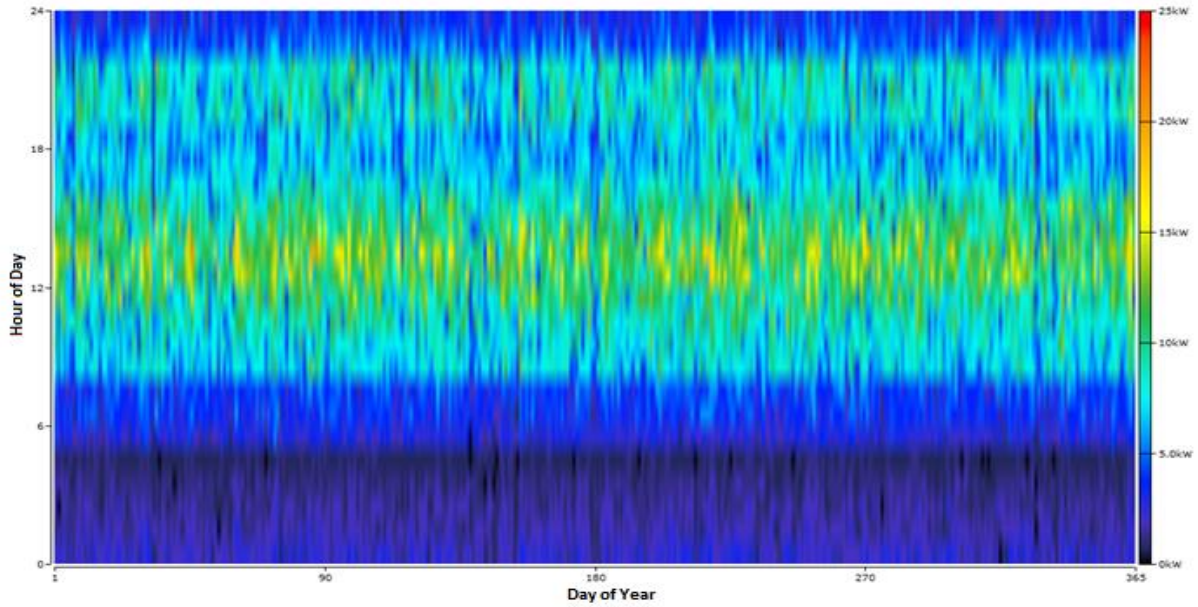

Fig. 7: Annual energy output

2.4 Economic assessment standards

The HOMER program optimizes costs based on a set of standards including net present costs, levelized energy costs, renewable energy rate, and ultimately the maximum amount of CO_2 emitted by the best system that HOMER has to offer.

2.4.1 Net present cost (NPC)

The NPC is determined by summing all program expenses throughout the system's duration and deducting any revenues earned. Equation (6) is utilized for this calculation, considering factors such as initial capital cost, replacement cost, operation and maintenance cost, fuel cost, etc.

$$\text{NPC} = \frac{C_{annual}.T_{ot}}{CRF(i, l_{project})} \quad (6)$$

where C_{annual}. Tot is the annualized cost; CRF represents the capital recovery factor; i is the interest rate and $l_{project}$ is the project life time.

2.4.2 Costs of energy (COE)

The cost of energy (COE) represents the portion of the overall project costs related to the electricity generated during a specific period. The inflation rate considered in this analysis is 5.0%. Equation (7) is used to determine the COE as outlined below:

$$\text{COE} = \frac{C_{annual}.T_{ot}}{E_{primary}.AC + E_{primary}.DC + E_{gridsales}} \quad (7)$$

where, $E_{primary}$ AC is the Primary AC load served; $E_{primary}$ DC is the Primary DC load served; $E_{gridsales}$ is absolute grid sales.

2.5 Sensitivity analysis

The HOMER algorithm iterates the sensitivity variable for the hybrid renewable energy system until the optimal result is achieved. Wind speed, solar radiation, inflation rate, and project life cycle cost are factors that are considered sensitive in this analysis. Concepts for hybrid renewable energy systems are presented in a table, ranking them from lowest to highest in terms of total net costs. Hybrid renewable energy systems with lower total net present costs (TNPC) are considered more favourable. The sensitivity analysis examines the impact of inputs on the results. HOMER-Pro has the capability to analyse confidential information in order to determine the optimal financial choice. It consists of decision variables as well as sensitivity

variables. Individuals are able to include a multitude of sensitive information for their analysis. Sensitivity factors can be utilized to present different sensitivity scenarios.

2.6 Optimization analysis

The system is simulated using HOMER-Pro, which subsequently presents a series of potential system configurations, arranged in order of increasing Net Present Cost (NPC) and excluding any unfeasible options. Employing a distinctive derivative-free approach, HOMER meticulously evaluates all feasible systems to determine the optimal solution. The optimal system design is characterized by having the fewest NPCs. Extensive knowledge of renewable energy sources, energy storage technologies, control strategies, and financial limitations is necessary for conducting a thorough HOMER analysis. The assessment criteria for HOMER include the Net Present Cost (NPC) and Cost of Energy (COE). HOMER defines Cost of Energy (COE) as the standard cost per kilowatt-hour of usable energy generated. The COE represents the average cost per kilowatt-hour of useful energy generated by the system. The HOMER software calculates the COE by dividing the annual energy production cost by the beneficial energy generated. Equation (6) can be utilized to compute the COE.

3. Results and discussion

3.1 Sensitivity analysis

The sensitivity analysis for various energy generation architectures, particularly Combined Cycle (CC) systems, is displayed as a screenshot in Table 1. Different inflation rates and project lifetimes are taken into account. The analysis covers expected inflation rates of 5%, 10%, and 15%, with project lifetimes ranging from 15 to 25 years. The Cost of Energy (COE) increases as the project lifetime extends and as the inflation rate decreases. For instance, with a 15% inflation rate, the COE rises from $1.17 at 15 years to $1.23 at 25 years. With a 10% and 5% inflation rate, the COE decreases from $1.34 to $1.33 and $1.54 at 15 years to $1.49 respectively at 25 years. The Net Present Cost (NPC) increases with longer project lifetimes and higher inflation rates. For example, when faced with a 15% inflation rate, the Net Present Cost (NPC) rises from $13,899 to $35,536 as the project's duration increases from 15 to 25 years. Elevated inflation rates typically result in higher NPC values, particularly for projects with longer lifespans (25 years). Additionally, the yearly operating expenses escalate with extended project durations and exhibit slight fluctuations across various inflation rates. Higher inflation rates and longer project lifetimes result in increased annual operating costs. The initial capital remains constant at $2,898 for all scenarios, except for one instance where it is $8,898. This indicates that the initial investment is consistent regardless of inflation rate and project lifetime, with the exception of one scenario highlighted red in Table 1. The production remained constant at 10.7 kWh/yr across all cases, suggesting that the production output is not influenced by the inflation rate or project lifetime. The Nominal Capacity stayed consistent at 544 kWh in all scenarios, indicating that this parameter remains unaltered. The sensitivity analysis assists in comprehending the effects of inflation and project duration on the total costs of a CC system, providing guidance on the most cost-effective and efficient operational configurations in various economic scenarios.

Table 1: Sensitivity analysis

Export All... | Sensitivity Cases — Left Click on a sensitivity case to see its Optimization Results. | Compare Economics

Sensitivity		Architecture					Cost			
Expected InflationRate (%)	Project Lifetime (years)					Dispatch	COE ($)	NPC ($)	Operating cost ($/yr)	Initial capital ($)
10.0	15.0					CC	$1.34	$10,843	$455.89	$2,898
10.0	20.0					CC	$1.33	$15,053	$498.45	$2,898
10.0	25.0					CC	$1.33	$19,704	$524.95	$2,898
15.0	15.0					CC	$1.17	$13,899	$194.47	$8,898
15.0	20.0					CC	$1.20	$22,984	$486.83	$2,898
15.0	25.0					CC	$1.23	$35,536	$521.88	$2,898
5.00	15.0					CC	$1.54	$8,619	$474.31	$2,898
5.00	20.0					CC	$1.51	$10,547	$507.34	$2,898
5.00	25.0					CC	$1.49	$12,202	$525.83	$2,898

3.2 Optimization

The screenshot Table 2 presents optimization results for various energy generation architectures, specifically Combined Cycle (CC) systems. The Cost of Energy (COE) is notably higher for the third option ($7.794) and the second option ($8.127) compared to the first option ($1.49). This suggests that the first system is the most cost-effective in terms of electricity generation. The Net Present Cost (NPC) is significantly higher for the second and third options (both at $4.02 billion) compared to the first option ($12,202). This indicates that the long-term costs of the second and third systems are considerably greater, possibly due to increased initial capital and operating expenses. The operating costs for the second and third options are significantly high ($1.00 million each) compared to the first option ($525.83 per year), further indicating that the first option is the most economical in terms of ongoing costs. The initial capital investment required for the second and third options, which amount to $4.00 billion each, is significantly higher than that of the first option, which totals $2,898. This suggests a substantial disparity in upfront costs. In the case of Production, the first option exhibits the lowest production capacity at 10.7 kWh per year, whereas the second and third options demonstrate significantly higher production levels at 38,759 kWh per year and 1,369 kWh per year, respectively. This suggests that the increased costs associated with the second and third options are warranted due to their higher energy output. The nominal capacity remains constant across all three systems at 544 kWh, indicating that this parameter is standardized. The first option is the most cost-effective, with the lowest levelized cost of energy (COE), net present cost (NPC), and operating costs, but it also has the lowest production capacity. The second and third options are considerably more costly, however, they provide significantly greater production capacities, making them potentially more suitable for larger-scale operations despite their higher price tags.

Table 2: The optimization results for various energy generation architectures

Export...

Optimization Results

Left Double Click on a particular system to see its detailed Simulation Results.

Architecture					Cost				SMA60-US	XANT21	LGChem9.8
				Dispatch	COE ($)	NPC ($)	Operating cost ($/yr)	Initial capital ($)	Production (kWh/yr)	Production (kWh/yr)	Nominal Capacity (kWh)
				CC	$1.34	$10,843	$455.89	$2,898	10.7		544
				CC	$5,817	$2.83B	-$67.0M	$4.00B		38,759	544
				CC	$5,760	$2.83B	-$67.0M	$4.00B	319	38,759	544

3.3 Cost summary

A comprehensive breakdown of the expenses linked to a particular energy system, classified by component and cost type is shown in Fig. 8. The costs are displayed in two formats: Net Present and Annualized. The information is currently configured to show Net Present costs. Additional categories of costs include Capital Costs, which refer to the initial investment needed to acquire and set up the components; Operating Costs, which are the ongoing expenses for operating and maintaining the system; Replacement Costs, which are the expenses associated with replacing components over the system's lifetime; and Salvage Value, which is the estimated residual value of components at the end of the project. Fuel costs are associated with fuel consumption, and in this system, they appear to be $0, indicating a renewable energy system without fuel expenses. The XANT M-21-ETR Wind Turbine is the most significant cost contributor, comprising the majority of the capital and operating costs. The LG Chem RESU10 battery possesses a negative salvage value, suggesting that disposal expenses will be accrued upon reaching the end of its lifespan. The Generic Large Converter and the SMA Sunny Tripower make smaller contributions to the total costs. The overall system cost is notably high, largely due to the presence of the wind turbine, underscoring the importance of evaluating the long-term economic sustainability of such a system (Fig. 8).

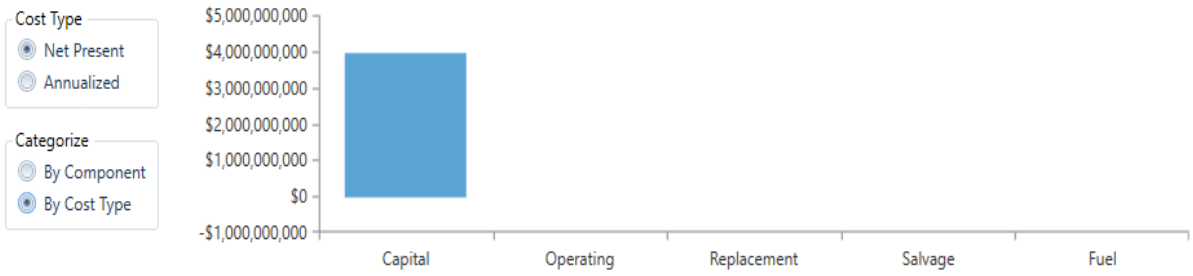

Component	Capital ($)	Replacement ($)	O&M ($)	Fuel ($)	Salvage ($)	Total ($)
Generic large, free converter	$2,500.00	$0.00	$8,846.80	$0.00	$0.00	$11,346.8
LGChem RESU10 [9.8kWh]	$375.00	$397.13	$132.70	$0.00	-$74.17	$830.6
SMA Sunny Tripower 60-US with Generic PV	$2,962.50	$0.00	$174.72	$0.00	$0.00	$3,137.2
XANT M-21-ETR [100kW]	$4,000,000,000.00	$0.00	$17,693,604.12	$0.00	$0.00	$4,017,693,604.1
System	$4,000,005,837.50	$397.13	$17,702,758.35	$0.00	-$74.17	$4,017,708,918.8

Fig. 8: A comprehensive assessment of the costs associated with specific energy system

3.4 Cash flow

A substantial $4,000,000.00 initial capital commitment is required as shown in Figure 9. The big green bar at year 0—which represents the initial expenses needed to set up the system—indicates this. The brown bars show that operating expenses are constantly negative and go from year 1 to year 25. These charges show that there will be continuous costs associated with operating and maintaining the system. The orange bars in years 10 and 20 indicate the particular periods at which replacement expenses arise. These expenses show that system components will eventually need to be replaced, increasing the overall cost for those years. A positive yellow bar indicates the salvage value at year 25. At the conclusion of the analysis time, this number represents the system components' residual value. The project appears to have considerable upfront expenditures, which are common for infrastructure and renewable energy projects given the size of the initial capital investment. Over the course of the system's lifespan, predictable and continuous maintenance and operating charges are shown by the comparatively steady operating costs. The replacement costs at years ten and twenty demonstrate how important it is to plan ahead and prepare for these recurring costs in order to guarantee system functionality. The system's salvage value at the conclusion of the analysis period shows that it is still somewhat valuable after 25 years, partially offsetting the total expenses.

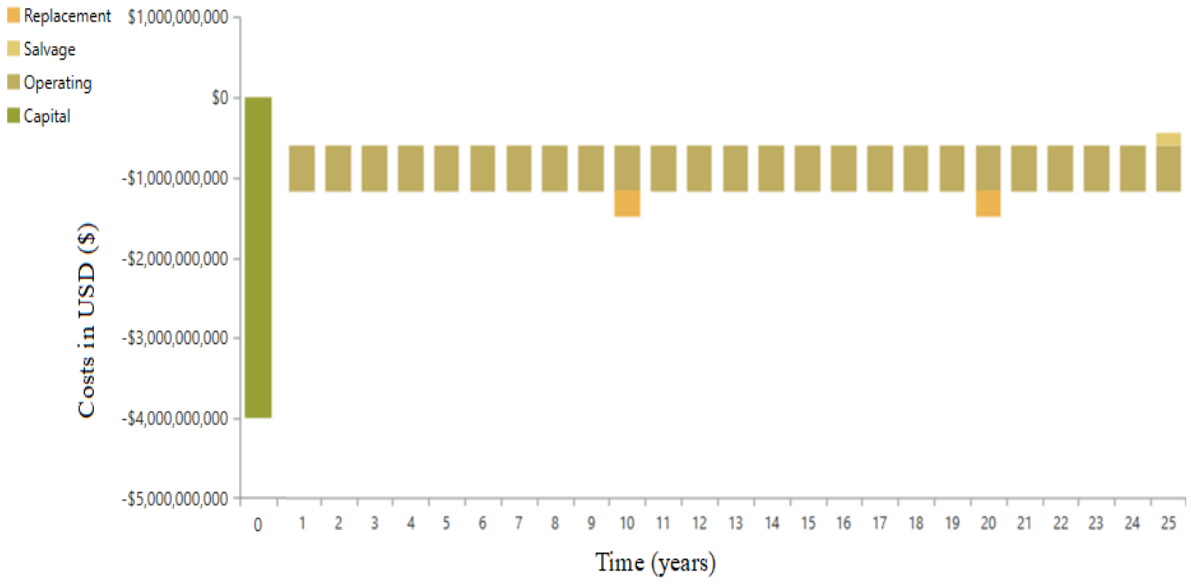

Fig. 9: A comparatively steady operating costs

3.5 Variability in average monthly electrical production

3.5.1 Variability in output power and total load served

Significant variability is observed in both total load served (brown) and wind output (blue) throughout the year in Fig. 10A. During Winter and Early Spring (January to March), wind output tends to be relatively lower, resulting in a greater reliance on alternative power sources to fulfil the load requirements. During the summer months of June to August, periods of increased wind output are observed, making a significant contribution to meeting the total load. Peaks in wind output are primarily seen during this season, suggesting stronger wind conditions during this time. A noticeable seasonal trend is observed in both total load served (brown) and solar output (orange) in Fig. 10B. During the winter months (January to March), lower solar output is noted, leading to increased dependence on alternative power sources to meet the load. During the summer months (June to August), there is a higher solar output observed, with the peak occurring around the middle of the year, indicating strong solar radiation during this period. The solar output follows a distinct seasonal pattern, with the highest output in the summer months and the lowest in the winter months. The seasonal variations of both wind and solar outputs are evident, with wind reaching its peak in the summer and solar peaking around mid-year. The total load served, represented by the colour brown, remains relatively consistent throughout the year, indicating that the integration of wind and solar power plays a significant role in meeting the demand. During periods of low wind and solar output, such as during the winter months, there may arise a requirement for supplementary power sources to fulfil the demand. Wind and solar power make substantial contributions to the overall load served, yet their effectiveness is greatly influenced by seasonal fluctuations.

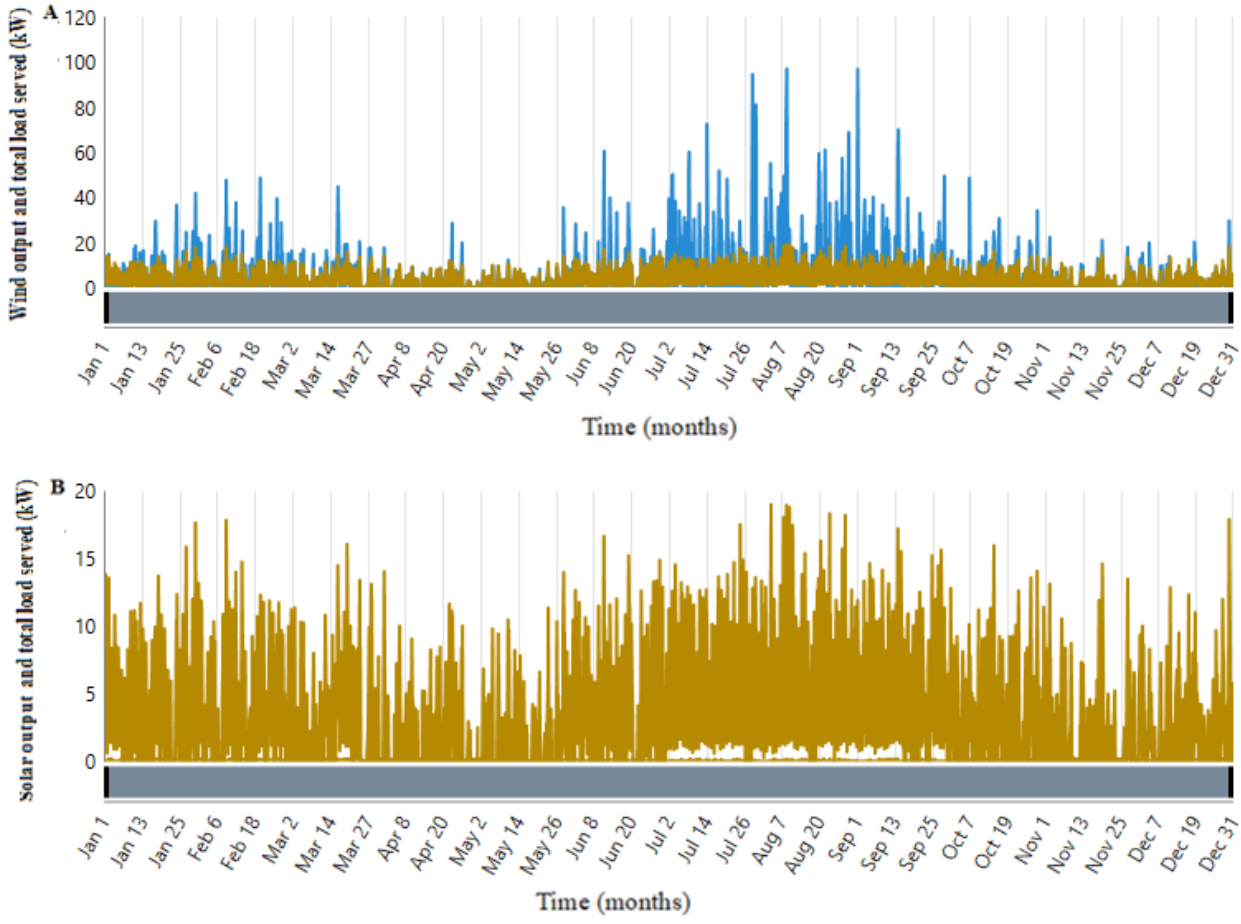

Fig. 10: Variability in output power and total load served

3.5.2 Variability study in total load served and unmet load/excess load

Significant variability is present in both the total load served (brown) and unmet load (blue) throughout the year, as illustrated in Fig. 11A. During the Winter and Early Spring (January to March), higher instances of unmet load (blue) indicate that the system faces challenges in meeting demand during these periods. During the summer months (June to August), there are fewer instances of unmet load and a more consistent total load served, indicating improved performance in meeting demand. There are distinct periods where demand exceeds supply, especially in the first half of the year. Fig. 11B demonstrates notable variability in both total load served (brown) and excess electricity (green). Throughout the Summer months (June to August), there is a discernible rise in excess electricity (green), signifying greater power generation in comparison to demand. During the Winter and Early Spring months (January to March), there are lower instances of excess electricity and more occurrences where the total load served (brown) meets the demand. Conversely, in the summer months, there is a notable surplus of electricity, indicating potential opportunities for energy storage or export. The system demonstrates improved performance during the summer months, exhibiting reduced unmet load and increased excess electricity. This observation implies that the power generation source, such as solar or wind energy, is more efficient during this period. Conversely, the higher unmet load during the winter and early spring months highlights the necessity for additional energy sources or enhanced capacity during these periods. The surplus electricity generated during the summer months underscores the potential for energy storage solutions to capture and utilize this excess during periods of increased demand.

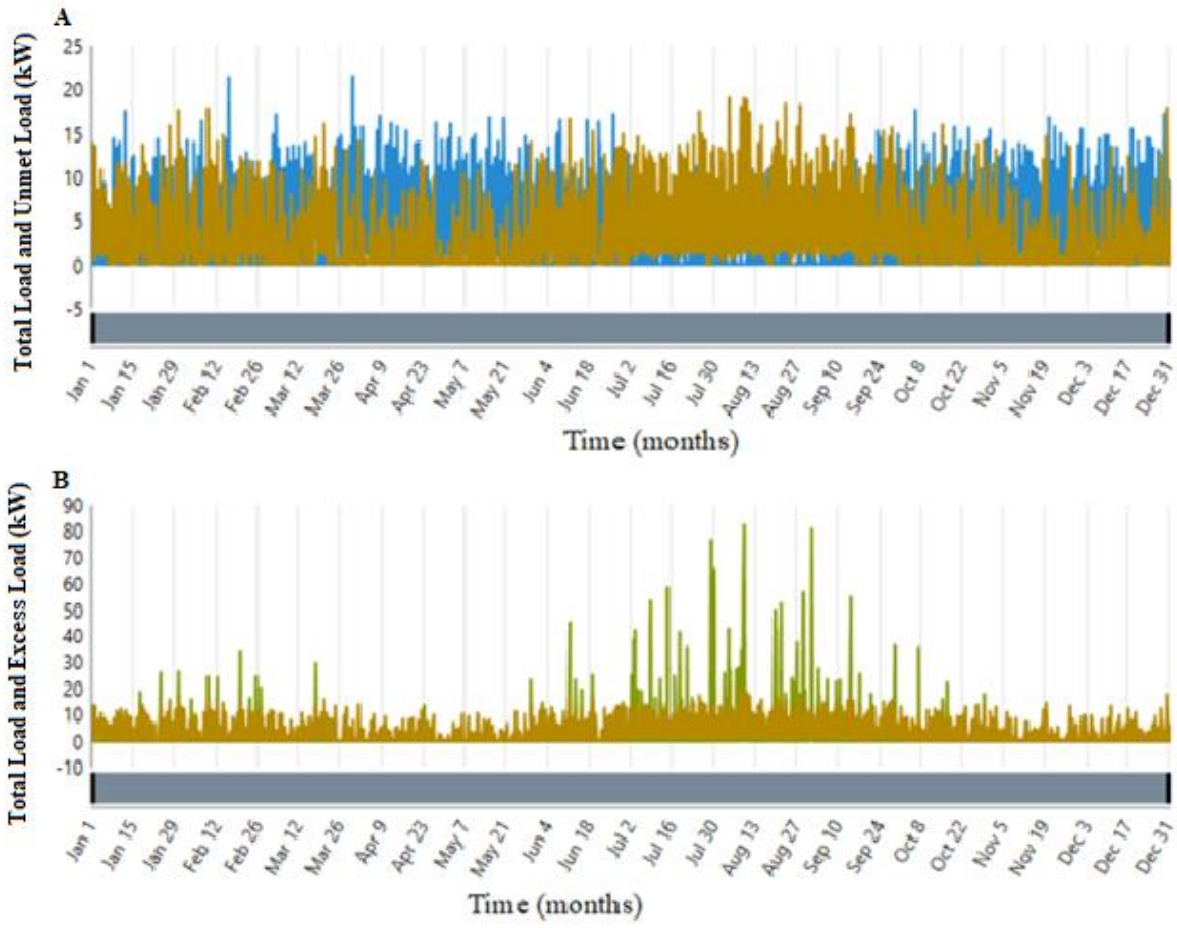

Fig. 11: Variability study in total load served and unmet load

3.5.3 Variability in total renewable power output and AC primary load

Fig. 12 comprises two graphs (A and B) illustrating the total renewable power output and AC primary load (in kilowatts, kW) over a span of time (months). Graph A displays the Total Renewable Power Output and AC Primary Load (kW), with the y-axis representing the power output and load values in kilowatts (kW) and the x-axis indicating the time in months, ranging from January 1st to December. The Total Renewable Power Output (green) represents the overall power generated from renewable sources, such as solar and wind, over a specific period. The AC Primary Load (purple) indicates the primary load demand for alternating current power during the same timeframe. Observations reveal that the total renewable power output experiences significant fluctuations throughout the year, with certain months, like mid-July to September, showing higher peaks. This phenomenon could be attributed to seasonal fluctuations impacting renewable energy production, such as heightened sunlight in the summer or increased wind speeds. The primary AC load seems to remain relatively stable, with occasional fluctuations that could align with shifts in energy demand or usage patterns. During certain periods, there is a notable surplus of renewable power output compared to the primary load, indicating a need for energy storage or export. Conversely, towards the end of the year, there is a more balanced relationship between renewable output and load.

Graph B displays the total renewable power output (green) and AC primary load served (blue). The total renewable power output represents the power generated from renewable sources over time, similar to Graph A. The AC primary load served is the amount of primary load demand that is fulfilled by renewable energy sources. It is noted that there is a consistent pattern in which the renewable power output closely aligns with the AC primary load served, particularly during periods of increased renewable output, such as July to September. The primary load served by the AC tends to be lower than the total output of renewable power, suggesting that not all generated renewable energy is being utilized to meet the load demand. This could indicate the presence of energy storage systems, exportation to the grid, or simply excess energy that is not being utilized. The overall pattern in this graph aligns with the seasonal trends observed in Graph A, showing an increase in renewable energy generation and consumption during the middle of the year. The fluctuations in renewable power output are a reflection of the variability in renewable energy sources, while the AC primary load remains relatively stable. The ability to supply the primary load with renewable energy varies, indicating the significance of energy management strategies such as storage, demand response, or grid integration to optimize the utilization of renewable energy sources. The data could prove to be beneficial for optimizing the balance between renewable energy supply and demand, enhancing energy storage solutions, or strategizing grid infrastructure to accommodate fluctuations in renewable energy generation.

3.6 Wind turbine output

The power output (kW) of the wind turbine is depicted in Figure 13. Red and yellow on the colour bar stand for higher power output (up to 100 kW). Lower power output is shown by blue (almost 0 kW). Different times of high and low power output were displayed on the graph. High output levels (yellow and red) happen occasionally and at various periods of the day and year. The high power output does not follow any discernible seasonal trend. Periods of high power production are dispersed throughout the year, suggesting that wind conditions may not be strictly seasonal but rather changeable. Periods of high power output are spaced out throughout the day. The wind power production varies during the day; there is no set daily pattern. Variability in wind power generation is indicated by the distribution of high and low values. There are noticeable low production periods (blue), which indicate periods when there is little to no wind power generated. It follows that there are erratic spikes and troughs in the amount of wind power generated. This suggests that the wind is not always constant. The wind turbine is only generating power at a small portion of its maximum capacity on average, as seen by the low capacity factor (4.42%). This may indicate inadequate wind conditions, the need for additional strategically placed or effective turbines, or both. The high levelized cost of $5,859/kWh suggests that the production of wind power is currently costly, maybe as a result of the high output fluctuation and low capacity factor.

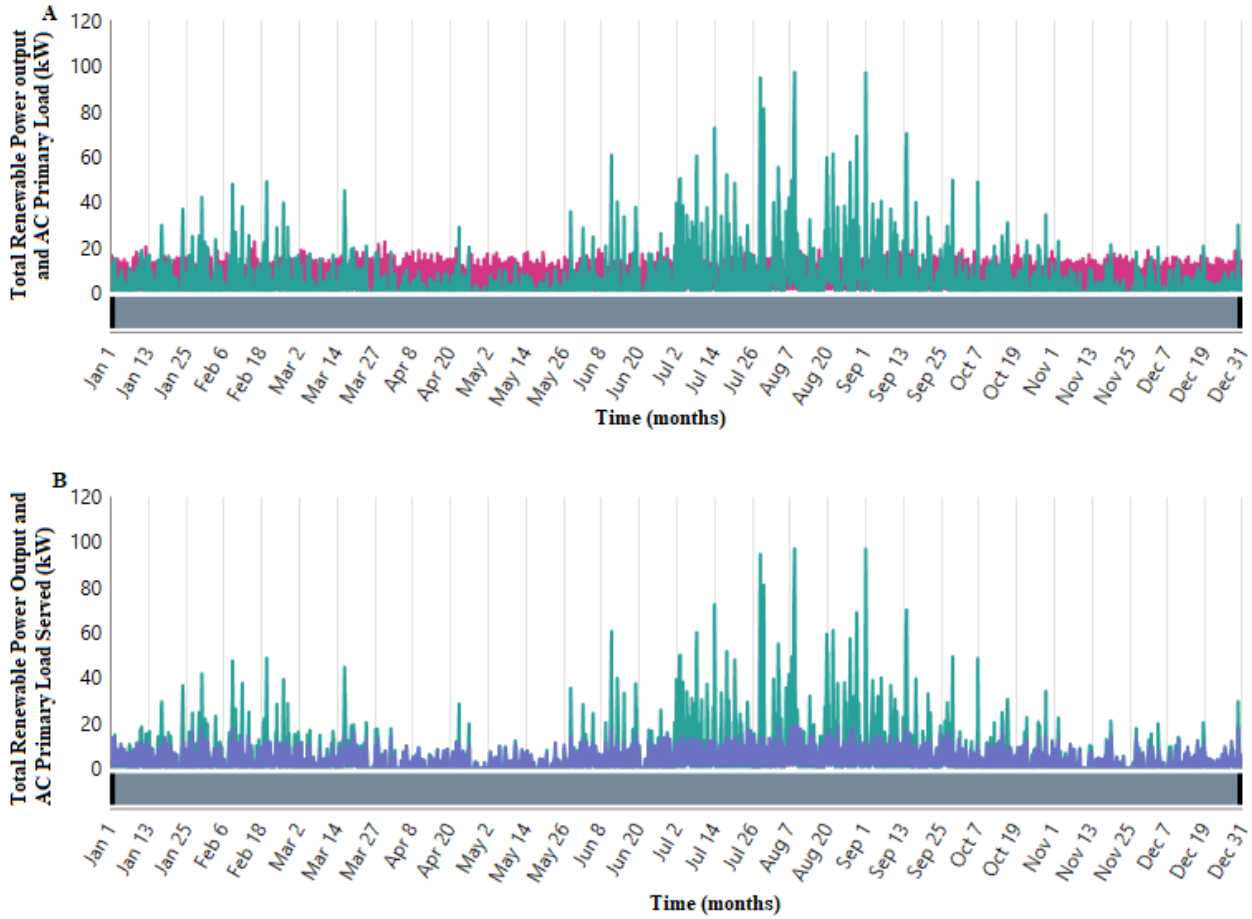

Fig. 12: Variability in total renewable power output and AC primary load

Quantity	Value	Units
Total Rated Capacity	100	kW
Mean Output	4.42	kW
Capacity Factor	4.42	%
Total Production	38,759	kWh/yr

Quantity	Value	Units
Minimum Output	0	kW
Maximum Output	96.9	kW
Wind Penetration	67.6	%
Hours of Operation	4,047	hrs/yr
Levelized Cost	5,859	$/kWh

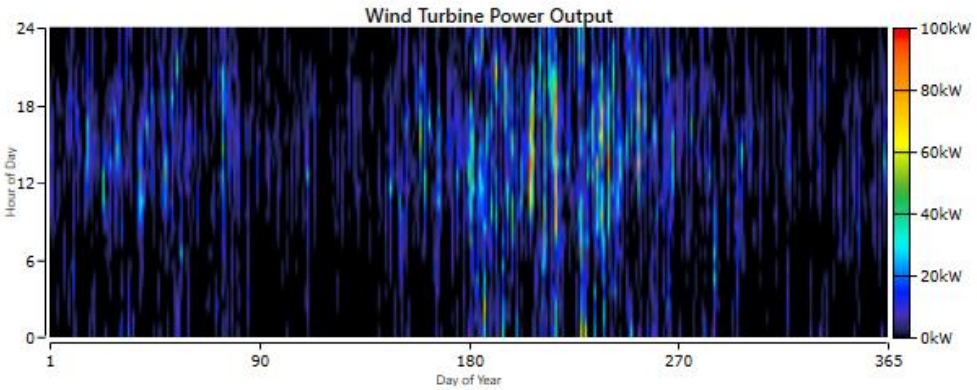

Fig. 13: The power output (kW) of the wind turbine

3.7 Solar power output

The PV power production is shown graphically in a heatmap (Fig. 14) that illustrates its annual variation by day and time of day. With a rated capacity of around 0.988 kW, the PV system generates 3.75 kWh on average per day. The PV system's ability to convert sunlight into energy is measured by its capacity factor, which stands at 15.8%. The PV system produces 1,369 kWh annually. The power outputs range from 0 kW to 0.997 kW at the minimum and highest, respectively. PV penetration, or the percentage of total energy that the PV system provides, is 2.39 percent. Every year, the system runs for 4,446 hours. The average cost per unit of energy generated during the course of the PV system's lifespan is reflected in the levelized cost of electricity from the system, which is 0.129 $/kWh. The heatmap offers a comprehensive glimpse at the year-over-year variations in the PV system's power production. Darker regions denote lesser power production, such as in the early morning, late evening, or on gloomy days, and bright yellow spots show higher power output, usually around noon when sun irradiation is maximum. This extensive data makes it possible to fully comprehend how well the PV system performs and may be utilized to design energy storage requirements, optimize operation, and assess economic feasibility.

Quantity	Value	Units
Rated Capacity	0.988	kW
Mean Output	0.156	kW
Mean Output	3.75	kWh/d
Capacity Factor	15.8	%
Total Production	1,369	kWh/yr

Quantity	Value	Units
Minimum Output	0	kW
Maximum Output	0.997	kW
PV Penetration	2.39	%
Hours of Operation	4,446	hrs/yr
Levelized Cost	0.129	$/kWh

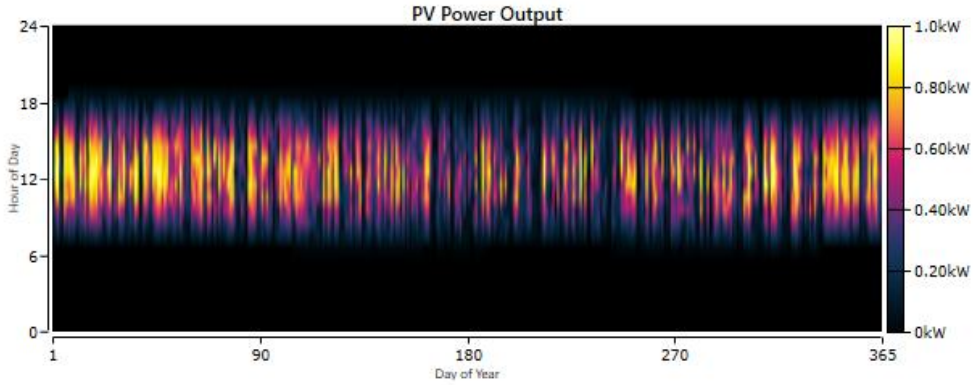

Fig. 14: The power output (kW) of the Solar PV System

3.8 State of charging

The heatmap displayed in Fig. 15 illustrates the state of charge throughout the year and across various hours of the day. The changes in colour signify the fluctuations in the state of charge over time. The distribution of the status of charge for each month is shown in the boxplot in the lower right corner. The whiskers show the range of the data, while the boxes show the interquartile range (IQR). Outliers would be shown as single points that are larger than the whiskers. Monthly fluctuations in the state of charge are seen, with larger fluctuations occurring in certain months. notably July and August. Sixty batteries overall, each having a 48V bus voltage and a notional capacity of 544 kWh, are linked in parallel strings to form the battery storage system. Only 489 kWh may be used, though. With a projected lifespan of ten years and a peak capacity of 111,055 kWh, the system can run independently for around 74.7 hours. With certain losses of 367 kWh annually, the energy input and production are balanced at 10,820–10,890 kWh annually. The boxplot and heatmap illustrate phases of greater and lower charge levels and offer insights into the daily and monthly fluctuations in the state of charge.

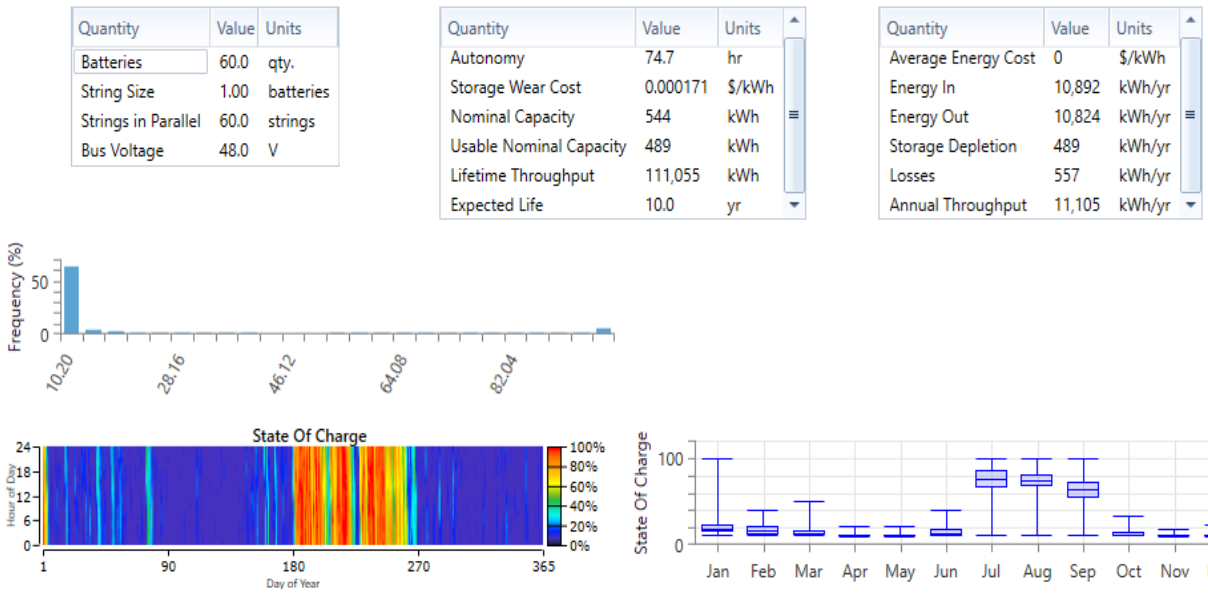

Fig. 15: The state of charge throughout the year and across various hours of the day

4. Conclusion

This study has effectively showcased the feasibility and advantages of incorporating photovoltaic (PV) solar and wind energy to address the electricity requirements of marginalized regions. The PV-wind hybrid system provides a sustainable, reliable, and economically viable solution for electrifying remote communities in Rivers State. The successful implementation of this system could potentially serve as a blueprint for comparable projects in different regions, aiding in the worldwide shift towards renewable energy and offering a route to energy self-sufficiency for isolated and underserved communities. Subsequent research efforts should concentrate on enhancing system components, investigating alternative renewable resources, and evaluating the scalability of this hybrid approach for wider applications.

References

Akinyele, D. (2018) Analysis of photovoltaic mini-grid systems for remote locations: A techno-economic approach. International Journal of Energy Research, 42(3): 1363-1380.

Alsharif M, (2017) Optimization design and economic analysis of energy management strategy based on photovoltaic/energy storage for heterogeneous cellular networks using the HOMER model. Solar Energy. 147(38).

Anigbata, V.A., Onah, T.O., and Nwankwo, A.M. (2022) Simulation of Prospects for Wind Turbine Power Generation in Nigeria Using Ashes. Uniport Journal of Engineering and Scientific Research, 6(2): 131-139.

Balachander, K, Kumaar, G.S., Mathankumar, M., Manjunathan, A. and Chinnapparaj, S. (2021) Optimization in design of hybrid electric power network using HOMER. Materials Today: Proceedings, 45: 1563-1567.

Das, H.S., Dey, A., Tan, C.W. and Yatim, A.H.M. (2016) Feasibility analysis of standalone PV/wind/battery hybrid energy system for rural Bangladesh. International Journal of Renewable Energy Research, 6(2): 402-412.

Dash, R.L., Mohanty, B. and Hota, P.K. (2023) Energy, economic and environmental (3E) evaluation of a hybrid wind/biodiesel generator/tidal energy system using different energy storage devices for sustainable power supply to an Indian archipelago. Renewable Energy Focus, 44: 357-372.

Fantidis, J., Bandekas, D. and Vordos, N. (2015) Study of a Wind/PV/Battery hybrid system - Case study at Plaka in Greece. Journal of Engineering Science and Technology Review. 8(3): 6-11.

Fulzele, J.B. and Daigavane, M.B. (2018) Design and optimization of hybrid PV-wind renewable energy system. Materials Today: Proceedings, 5(1): 810-818.

Giannetti, B.F., Agostinho, F., Almeida, C.M., Liu, G., Contreras, L.E., Vandecasteele, C. and Poveda, C. (2020) Insights on the United Nations Sustainable Development Goals scope: Are they aligned with a ‘strong’sustainable

development. Journal of Cleaner Production, 252: 119574.

Givler, T. and Lilienthal, P. (2005) Using HOMER® Software NREL's Micropower Optimization Model to Explore the Role of Gensets in Small Solar Power Systems. A national laboratory of the U.S. Department of Energy Office of Energy Efficiency & Renewable Energy. Report number: TP-710-36774.

Gul, E., Baldinelli, G., Bartocci, P., Bianchi, F., Piergiovanni, D., Cotana, F. and Wang, J. (2022) A techno-economic analysis of a solar PV and DC battery storage system for a community energy sharing. Energy, 244: 123191.

IEA (International Energy Agency) (2010) Energy poverty: how to make modern energy access universal? Retrieved from https:// www. undp.org/content/undp/en/home/librarypage/environment-energy/sustainable_energy/energy_ poverty_ howtomakemodernenergyaccess universal.html.

IEA (International Energy Agency) (2019a) Energy Access (database), IEA. Retrieved from https://www.iea.org/sdg/electricity/, accessed 18 October 2019.

IEA (2023c) World Energy Investment 2023. Retrieved from https://www.iea.org/reports/world-energy-investment-2023

Khalil, L., Bhatti, K.L., Awan, M.A.I., Riaz, M., Khalil, K. and Alwaz, N. (2021) Optimization and designing of hybrid power system using HOMER pro. Materials Today: Proceedings, 47: S110-S115.

Li, C., Zhou, D., Wang, H., Lu, Y. and Li, D. (2020) Techno-economic performance study of stand-alone wind/diesel/battery hybrid system with different battery technologies in the cold region of China. Energy, 192: 116702.

Lilienthal, P. and Lambert, T. (2004) HOMER The Micropower Optimization Model. A national laboratory of the U.S. Department of Energy Office of Energy Efficiency & Renewable Energy. Report number: FS-710-35406.

Maren, I.B., Adisa, A.B., Dandakouta, H. and Ejilah, R.I. (2024) Performance Evaluation of a Hybrid Solar-Wind Power System for Heipang Community Load Demand. Arid Zone Journal of Engineering, Technology and Environment, 20(1): 305-324.

Reichling, J. and Kulacki, F. (2008) Utility scale hybrid wind-solar thermal electrical generation: A case study for Minnesota. Energy, 33(4): 626-638.

Saha, P., Kar, A., Behera, R.R., Pandey, A., Chandrasekhar, P. and Kumar, A. (2022) Performance optimization of hybrid renewable energy system for small scale micro-grid. Materials Today: Proceedings, 63: 527-534.

Sarkar, J. and Khule, S. (2016) A study of MPPT schemes in PMSG based wind turbine system. International Conference on Electrical, Electronics, and Optimization Techniques (ICEEOT). Chennai, India, 1: 100–105.

Sanni, S., Ibrahim, M. and Mahmud, I. (2016) Potential of Off-grid Solar PV/Biogas Power Generation System: Case Study of Ado Ekiti Slaughterhouse. International Journal of Renewable Energy Research, 9(3): 1309-1318.

Sofimieari, I., Bin-Mustafa, M. and Obite, F. (2019) Modelling and analysis of a PV/wind/diesel hybrid standalone microgrid for rural electrification in Nigeria. Bulletin of Electrical Engineering and Informatics, 8(4): 1468-1477.

Tigabu, M., Guta, D. and Admasu, B. (2019) Economics of Hydro-Kinetic Turbine for off-grid Application: A Case Study of Gumara River, Upper Blue Nile, Amhara, Ethiopia. International Journal of Renewable Energy Research, 9(3):1368-1375.

USAID (2020) Nigeria power Africa Fact sheet. Retrieved from https://www.usaid.gov/ powerafrica/nigeria.

Vendoti, S., Muralidhar, M. and Kiranmayi, R. (2018) HOMER based optimization of solar-wind-diesel hybrid system for electrification in a rural village. In 2018 International Conference on Computer Communication and Informatics (ICCCI) (pp. 1-6). IEEE.

Wang, C., Xia, M., Wang, P. and Xu, J. (2022) Renewable energy output, energy efficiency

and cleaner energy: Evidence from non-parametric approach for emerging seven economies. Renewable Energy, 198: 91-99.

WHO (2016) Burning opportunity: clean household energy for health, sustainable development, and wellbeing of women and children. Retrieved from http://apps.who.int/iris/bitstream/handle /10665/ 204717/9789241565233_eng.pdf.

WHO (2020) Proportion of population with primary reliance on clean fuels and technologies (%). Retrieved from https://www.who.int/data/gho/ data/indicators/indicator-details/GHO/ proportion-of- population-with -primary-reliance-on-clean-fuels-and-technologies-(-.

World Bank (2019) World Bank Enterprise Surveys. Retrieved from www.enterprise surveys.org/, accessed 1 September 2019

World Bank (2020a) Access to electricity (% of pop ulation). Retrieved from https://data. worldbank .org/ indicator/ EG.ELC.ACCS.ZS.

World Bank (2023) Tracking SDG 7: The Energy Progress Report. Retrieved from https:// trackingsdg7. esmap.org/